Available online at www.sciencedirect.com
ScienceDirect
Journal of the European Ceramic Society 29 (2009) 751–756
www.elsevier.com/locate/jeurceramsoc

Microstructural, structural and electrical properties of La^{3+}-modified $Bi_4Ti_3O_{12}$ ferroelectric ceramics

V.B. Santos [a], J.-C. M'Peko [a,*], M. Mir [b], V.R. Mastelaro [a], A.C. Hernandes [a]

[a] *Instituto de Física de São Carlos (IFSC), Universidade de São Paulo (USP), C. Postal: 369, 13560-970 São Carlos, São Paulo, Brazil*
[b] *Departamento de Ciências Exatas, Universidade Federal de Alfenas (UNIFAL-MG), Rua Gabriel Monteiro da Silva 714, CEP: 37130-000 Alfenas, Minas Gerais, Brazil*

Received 12 January 2008; received in revised form 3 June 2008; accepted 13 June 2008
Available online 12 August 2008

Abstract

$Bi_{4-x}La_xTi_3O_{12}$ (BLT) ceramics were prepared and studied in this work in terms of La^{3+}-modified microstructure and phase development as well as electrical response. According to the results processed from X-ray diffraction and electrical measurements, the solubility limit (x_L) of La^{3+} into the $Bi_4Ti_3O_{12}$ (BIT) matrix was here found to locate slightly above $x = 1.5$. Further, La^{3+} had the effect of reducing the material grain size, while changing its morphology from the plate-like form, typical of BIT ceramics, to a spherical-like one. The electrical results presented and discussed here also include the behavior of the temperature of the ferroelectric–paraelectric phase transition as well as the normal or diffuse and/or relaxor nature of this transition depending on the La^{3+} content.

Keywords: Sintering; Microstructure-final; Electrical properties; Ferroelectric properties; $Bi_4Ti_3O_{12}$-based compound

1. Introduction

Bismuth titanate ($Bi_4Ti_3O_{12}$, BIT) is a ferroelectric material with wide potential application in the electronic industry as capacitors, memory devices and sensors, and the simplest compound in the Aurivillius family which consists of $(Bi_2O_2)^{2+}$ sheets alternating with $(Bi_2Ti_3O_{10})^{2-}$ perovskite-like layers stacked along the crystallographic c direction.[1,2] In order to improve the electrical properties of BIT, solid solutions with other cations have been considered and explored. This is the case of the La^{3+}-doped BIT ($Bi_{4-x}La_xTi_3O_{12}$, BLT) system which has shown to improve, for $x = 0.75$ for instance, the fatigue endurance of the resulting material upon repeated cyclic electric fields.[3] This and other results have revived interest in properties of the BLT solid solutions. Nevertheless, in spite of the various studies that can be found so far in the literature on this system, see, e.g. Refs. [3–9] there appears to be no comprehensive work in which its main features, namely La^{3+}-assisted sintering process and microstructure development, La^{3+} tolerance, long-range order structural and electrical properties, have been all together collected and correlatively investigated. This is the purpose of the present work where the study of BLT ceramic materials has been reconsidered. Important aspects such as solubility limit of La^{3+} into BIT, microstructure and phase development, and resulting ferroelectric characteristics are closely revisited in a correlative fashion.

2. Experimental procedure

The studied materials were prepared through the conventional ceramic method starting from high-purity raw materials (from Alfa Aesar): Bi_2O_3 (99.5%), La_2O_3 (99.999%), and TiO_2 (99.9%). Powders from these oxides were mixed according to the formula $[2-(x/2)]Bi_2O_3 + (x/2)La_2O_3 + 3TiO_2 \rightarrow Bi_{4-x}La_xTi_3O_{12}$, where $x = 0$, 0.5, 0.75, 1, 1.5 and 2, hereafter labeled as BLT100x, i.e., BLT000 ≡ BIT, BLT050, BLT075, BLT100, BLT150 and BLT200, respectively. The mixtures were ball-milled for 36 h in polyethylene vases while dispersed in isopropyl alcohol. The applied calcination (temperature and time) parameters are indicated in Table 1. These were optimized so as to obtain starting single- or almost single-phase powders, according to X-ray diffraction (XRD)

* Corresponding author.
E-mail address: peko@if.sc.usp.br (J.-C. M'Peko).

0955-2219/$ – see front matter © 2008 Elsevier Ltd. All rights reserved.
doi:10.1016/j.jeurceramsoc.2008.06.025

Table 1
Calcination and sintering (temperature/time) parameters (C.P. and S.P., respectively), measured densities (ρ_{meas}), theoretical densities (ρ_{theo}), relative densities and average grain size (D) of all the prepared BLT samples

Composition	C.P. (°C/h)	S.P. (°C/h)	ρ_{meas} (g/cm^3)	ρ_{theo}[a] (g/cm^3)	ρ_{meas}/ρ_{theo} (%)	D (μm)
BIT	800/3	1050/2	7.722	8.044^{OR}	96.00	3.0
BLT050	800/3	1180/2	7.522	7.799^{MO}	96.44	1.6
BLT075	860/6	1195/2	7.274	7.688^{MO}	94.61	1.5
BLT100	860/6	1180/3	7.082	7.575^{MO}	93.49	1.4
BLT150	880/6	1250/5	7.040	7.333^{TE}	95.99	1.2
BLT200	880/6	1310/5	7.037	7.327^{TE}[b]	96.04	2.0

[a] Values estimated from the corresponding XRD patterns (see text). The super-index quoted on the reported values responds to the crystallographic symmetry (orthorhombic; OR, monoclinic; MO, or tetragonal; TE) from which the better fitting results were obtained.
[b] Value estimated assuming the unit cell mass of the BLT150 composition according to the result of solubility limit processed from the XRD analysis (see text).

data collected using a Rigaku-Rotaflex RU-200B diffractometer (50 kV × 100 mA) with Cu Kα (λ = 1.5405 Å). In the following, the powders were again ball-milled for 12 h in the above plastic recipients with isopropyl alcohol. Shrinkage measurements were carried out in a Netzsch Dil 402 PC dilatometer on pressed powders, the results from which an optimal sintering temperature to be applied in an attempt to obtain highly dense bodies was evaluated for each BLT composition. The sintering (temperature and time) parameters thus finally considered are also indicated in Table 1. The values of the ceramics density were measured through the Archimedes method. In addition, scanning electron microscopy (SEM) observations, accomplished in a Zeiss DSM960 microscope, and XRD measurements of the ceramic materials were conducted in order to evaluate the La^{3+}-induced microstructure and structure development features involved. Finally, electrical measurements were carried out in a Solartron SI 1260 impedance analyzer at different selected frequencies: 10 kHz, 100 kHz and 1 MHz, over a wide temperature range up to about 700 °C, and using Pt as electrodes diffused onto the samples' surfaces. From these measurements, permittivity and dielectric losses of all the ceramic samples were processed.

3. Results and discussion

Fig. 1 shows the room temperature XRD patterns of all the calcined BLT powders. These are characterized by reflection peaks isostructural with $Bi_4Ti_3O_{12}$. Moreover, according to the calcination (annealing temperature and time) parameters applied (see Table 1), some low-intensity, additional peaks associated to impurity $La_2Ti_2O_7$ (L2T2), La_2TiO_5 (L2T1) and $Bi_2Ti_2O_7$ (B2T2) phases were detected in the XRD pattern from the BLT200 composition. The results of thermal shrinkage obtained from the dilatometric analysis of samples prepared from the calcined powders are shown in Fig. 2 in terms of $\Delta L/L_o$ (left scale) and its derivative $d(\Delta L/L_o)/dT$ (right scale). The samples start to shrink above about 800 °C and undergo a maximum shrinkage rate from close to about 1200 °C above, depending on composition. The sintering temperatures finally considered (see also Table 1) were selected according to each composition-dependent temperature of maximum shrinkage rate (minimum values of $d(\Delta L/L_o)/dT$), except for the well studied BIT system, whose melting process is known to occur at about 1210 °C and for

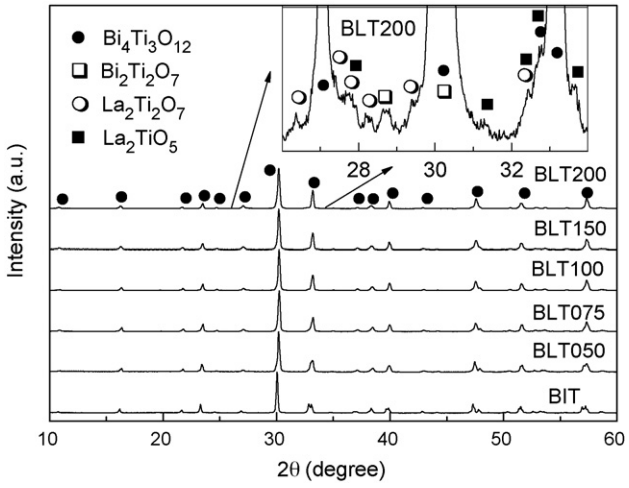

Fig. 1. XRD patterns of the calcined $Bi_{4-x}La_xTi_3O_{12}$ (BLT100x) powders. All the patterns show peaks corresponding to a phase isostructural with $Bi_4Ti_3O_{12}$ (JCPDS: 35-0795). For $x = 2.0$, additional low-intensity phases isostructural with $La_2Ti_2O_7$ (JCPDS: 81-1066), $Bi_2Ti_2O_7$ (JCPDS: 32-0118) and La_2TiO_5 (JCPDS: 75-2394) were identified.

which, following the literature,[10,11] a relatively low temperature of 1050 °C was assumed to be enough to obtain a dense material. The values of density measured (ρ_{meas}) for all the ceramic samples are given in Table 1. These reveal relatively high when compared to the expected theoretical density values (ρ_{theo}) that

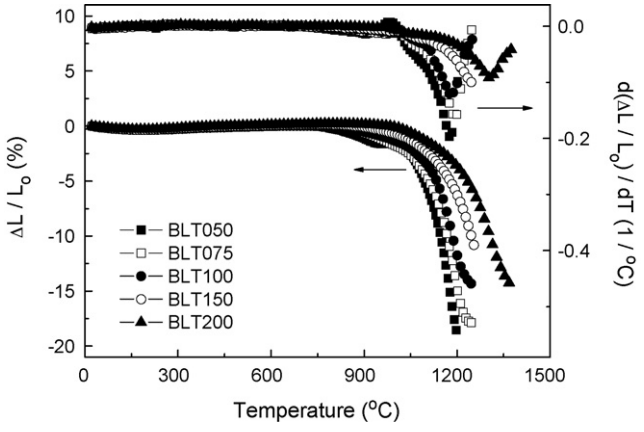

Fig. 2. Results of thermal shrinkage from the dilatrometric measurements conducted on compacted $Bi_{4-x}La_xTi_3O_{12}$ (BLT100x) powders, and presented in terms of $\Delta L/L_o$ (left scale) and $d(\Delta L/L_o)/dT$ (right scale).

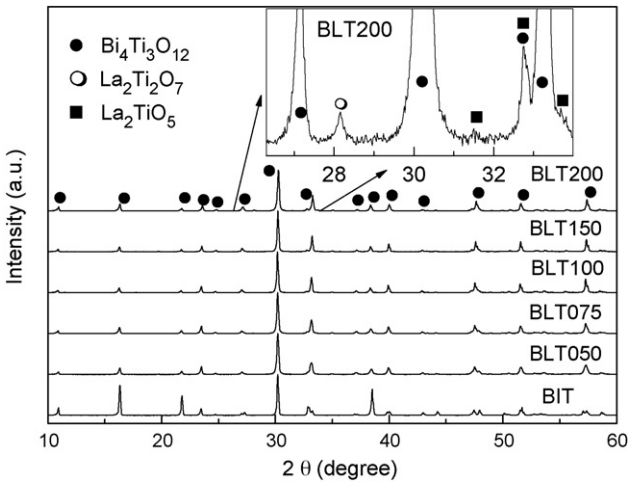

Fig. 3. XRD patterns of the sintered $Bi_{4-x}La_xTi_3O_{12}$ (BLT100x) samples. Again (as in Fig. 1), all the patterns show peaks corresponding to a phase isostructural with $Bi_4Ti_3O_{12}$ (JCPDS: 35-0795). For $x = 2.0$, additional low-intensity phases isostructural with $La_2Ti_2O_7$ (JCPDS: 81-1066) and La_2TiO_5 (JCPDS: 75-2394) were still identified.

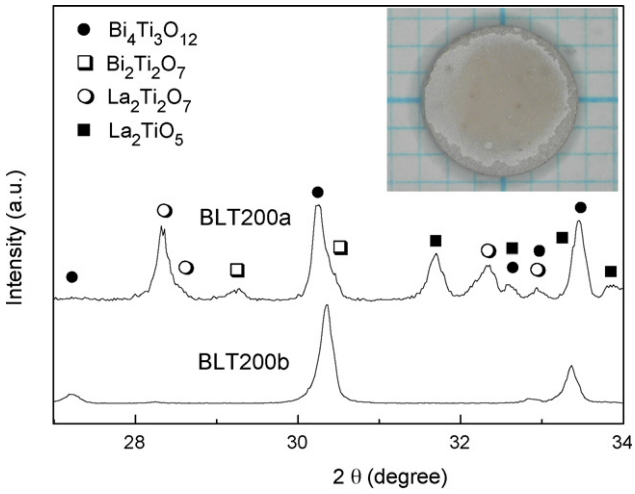

Fig. 4. Full-intensity XRD patterns from the BLT200 sample before (BLT200a) and after (BLT200b) removing the powder accumulated at the surface sample from sintering. A picture of the as-sintered sample is included.

were estimated from the XRD results, as explained later. The possibility of achieving sintering of the BLT samples at temperatures quite close to and above 1210 °C indicates that presence of La^{3+} has the effect of increasing the melting temperature of the original BIT compound.

Fig. 3 shows the room temperature XRD patterns of all the samples after sintering. The results are similar to those of Fig. 1, with the particularity that presence of some impurity traces associated now only to L2T2 and L2T1 still persisted for the BLT200 composition. At this time, the solubility limit (x_L) of La^{3+} into $Bi_4Ti_3O_{12}$ so as to give the stoichiometric formula $Bi_{4-x}La_xTi_3O_{12}$ should be proposed as $x_L < 2.0$. This statement is further supported by the observation according to which, during sintering, a compact thin layer of a white-like powder accumulated around the BLT200 sample surface. The XRD pattern illustrated in Fig. 3 for the BLT200 sample was recorded after removing this powder layer. For the sake of a comparison, Fig. 4 shows the full-intensity XRD results corresponding to the sintered BLT200 sample before (BLT200a) and after (BLT200b) removing the surface excess powder. A picture of the as-sintered sample (BLT200a) has been also included. Presence of the three original impurity phases, i.e., L2T2, L2T1 as well as B2T2, is detected for BLT200a. According to the literature, B2T2 melts at 1250 °C,[12] a value of which should increase if La^{3+} cations are involved. All these observations suggest that sintering of the BLT200 composition involved the development of a liquid phase from a $Bi_2Ti_2O_7$-based phase. The formation of the white-like powder layer around the BLT200 surface sample should thus result from the elimination process of the liquid phase during the sample densification.

Fig. 5 shows the SEM micrographs from the BIT, BLT075 and BLT200 samples, and summarizes well the general La^{3+}-induced microstructural features of the samples during sintering. That is, while the starting ceramic sample of BIT shows grains with the usual plate-like form, these undergo a transformation to a spherical form with adding and increasing La^{3+} into the BIT system. The average values of grain size directly determined from the SEM micrographs, by using the classical linear intercept method,[13] are also given in Table 1 for all the studied compositions. A process of grain growth inhibition is observed as La^{3+} is added to the BIT system up to $x = 1.5$, after which the grain size augments for a further increase of La^{3+} to $x = 2.0$. The grain growth inhibition should be viewed as a result of the development of a grain-boundary pinning process induced by the own presence of (substitutional and/or interstitial) La^{3+} ions at the grain surface.[14] Besides involving the application of a higher sintering temperature, the increase of grain size from $x = 1.5$ to $x = 2.0$ appeared to specially involve the presence of the liquid phase during the sintering process, as it usually happens in the synthesis of many other ceramic systems.[15,16]

Fig. 6 illustrates the temperature dependence of permittivity for sintered ceramics of BIT, BLT075 and BLT100 measured at 100 kHz. The curves show dielectric peaks that correspond to the ferro- to paraelectric phase transition expected in ferroelectric materials. Moreover, from $x = 1.0$ above, the phase transition was seen to change from normal (sharp-like dielectric peak) to diffuse (broad-like dielectric peak). For all the studied samples, the room temperature values of permittivity (ε_{RT}) and dielectric losses ($\tan\delta_{RT}$) as well as the temperature values of maximum permittivity (T_m) are given in Table 2. All these values compare well with those values typically found in the literature for BIT-based ferroelectric materials.[7,9,17] In particular, the values of T_m are also plotted in Fig. 7 for better visualizing the behavior of this parameter upon variation of the La^{3+} content. It is seen that T_m significantly decreases as La^{3+} increases up to $x = 1.5$, after which the T_m variation turns relatively insignificant. As previously noted in the literature,[6,7] different from the results extrapolated in BIT compounds doped with diverse rare-earth cations ($Bi_{4-x}R_xTi_3O_{12}$; R = rare earth), where T_m was proposed to vary monotonically as a linear function of the rare-earth content,[4] variation of T_m with La^{3+} does not really reveal such a linear behavior trend when extending further the composition range of study. Of special interest for this work, what is

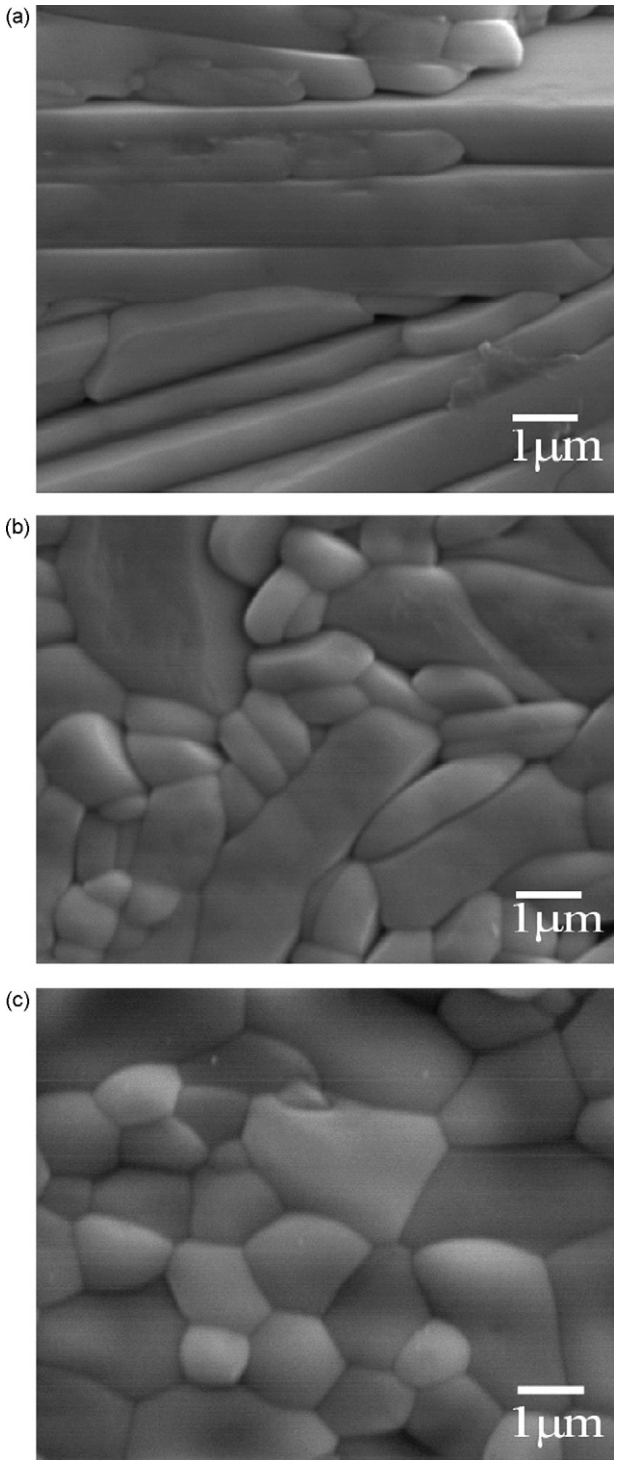

Fig. 5. SEM micrographs of the sintered: (a) $Bi_4Ti_3O_{12}$ (BIT), (b) $Bi_{3.25}La_{0.75}Ti_3O_{12}$ (BLT075) and (c) $Bi_2La_2Ti_3O_{12}$ (BLT200) samples.

important to observe from the T_m-versus-composition figure is that the solubility limit of La^{3+} into BIT, initially proposed as $x_L < 2.0$ following the XRD results, should be actually regarded as approaching $x_L \cong 1.5$. The small variation still observed for T_m from BLT150 to BLT200 (Table 2) however suggests that x_L should indeed be slightly higher than 1.5.

From the crystallographic viewpoint, on the other hand, there is a general agreement in the literature that the lattice symmetry of BIT-based compounds is tetragonal (TE) above T_m in the paraelectric phase.[1,2,5,18] Meanwhile, below T_m in the ferroelectric phase, BIT-based compounds have been treated as either orthorhombic (OR) or monoclinic (MO),[1,2,4,18–20] provided that the deviation between both systems is in this case small and often hardly detectable. In the present work, we chose to fit the exper-

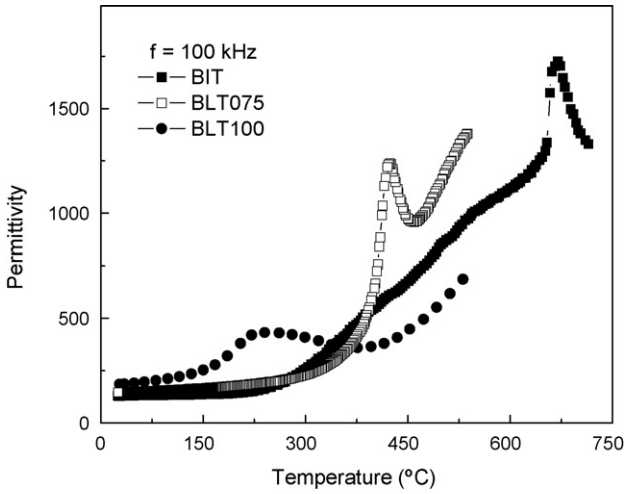

Fig. 6. Temperature dependence of permittivity measured for the sintered $Bi_4Ti_3O_{12}$ (BIT), $Bi_{3.25}La_{0.75}Ti_3O_{12}$ (BLT075) and $Bi_3LaTi_3O_{12}$ (BLT100) samples.

Table 2
Temperature of maximum permittivity (T_m), room temperature permittivities and dielectric losses (ε_{RT} and $\tan\delta_{RT}$, respectively) of all the prepared BLT ceramic samples

Composition	T_m (°C)[a]	ε_{RT}	$\tan\delta_{RT}$
BIT	670	130	0.022
BLT050	508	145	0.023
BLT075	424	147	0.024
BLT100	246	186	0.022
BLT150	−137	168	0.017
BLT200	−149	101	0.014

[a] Values corresponding to the data processed at 100 kHz.

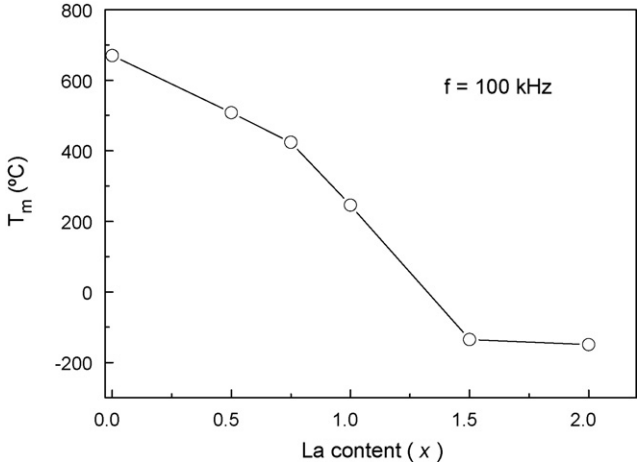

Fig. 7. Dependence of the temperature of maximum permittivity (T_m) of the sintered BLT100x samples upon variation of the La^{3+} content.

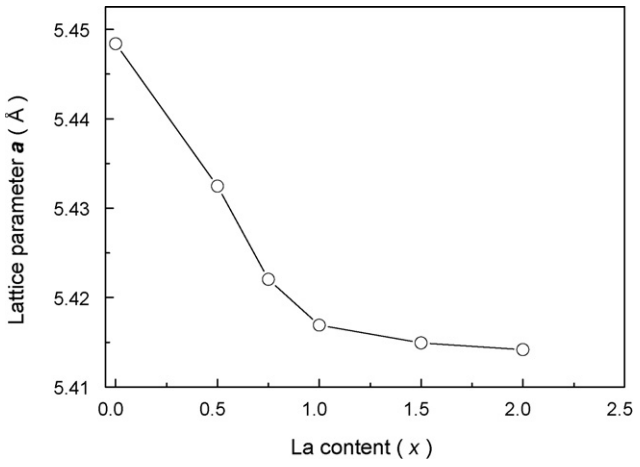

Fig. 8. Dependence of the calculated lattice parameter a of the sintered BLT100x samples upon variation of the La^{3+} content. For $x = 1.5$ and $x = 2.0$, the parameters were converted from tetragonal to orthorhombic just for comparison with the other sample data (see text).

imental XRD patterns of the prepared BLT ceramics through the "Le Bail" method,[21] using the professional Full Proof program, from which the values of lattice parameters (a, b, c, α, β and γ) and resulting volume (V) were automatically obtained. The values of theoretical density (ρ_{theo}) reported in Table 1 were estimated from the values of unit cell mass and volume, where $V_{TE} = a^2c$, $V_{OR} = abc$ and $V_{MO} = abc \sin\beta$.[22] As the solubility limit (x_L) of La^{3+} into BIT finally resulted slightly higher than $x = 1.5$, that is, according to the electrical measurements (T_m), one should thus conclude that the value of theoretical density given in Table 1 for the BLT200 sample (to which we attributed the unit cell mass of BLT150) was indeed slightly over-estimated.

In special, Fig. 8 shows the behavior of the estimated lattice parameter a upon variation of the La^{3+} content. For a better comparison with the orthorhombic and monoclinic data, the estimated values of a_{TE} from the BLT150 and BLT200 samples (that showed TE symmetry at room temperature) were converted into the equivalent a_{OR} applying the relation $a_{OR} = \sqrt{2}a_{TE}$.[8] Keeping in mind that from the XRD results the solubility limit (x_L) of La^{3+} into BIT falls below $x = 2.0$, Fig. 8 ratifies the observation finally deduced from the electrical results in the sense that x_L should situate close to but slightly above $x = 1.5$. At this time, it is important to point out that the location of x_L, as estimated here from considering XRD as well as electrical measurements, lies below an earlier value of $x_L = 2.8$ reported in the literature for the BLT formulation,[4,5] a result about which we could not find however any independent, similar statement. It is unlike to evaluate the total preciseness of that x_L value provided that the purity grades of the used raw materials were not given in those Refs. [4,5]. We could just speculate that those starting materials were perhaps less pure than the ones used in this work.

Finally, Fig. 9 shows the temperature dependence of permittivity for sintered ceramics of BLT100 (Fig. 9a) and BLT150 (Fig. 9b) measured at three different frequencies. In general, no frequency dispersion was observed for the permittivity behavior around the transition temperature in the BLT samples with

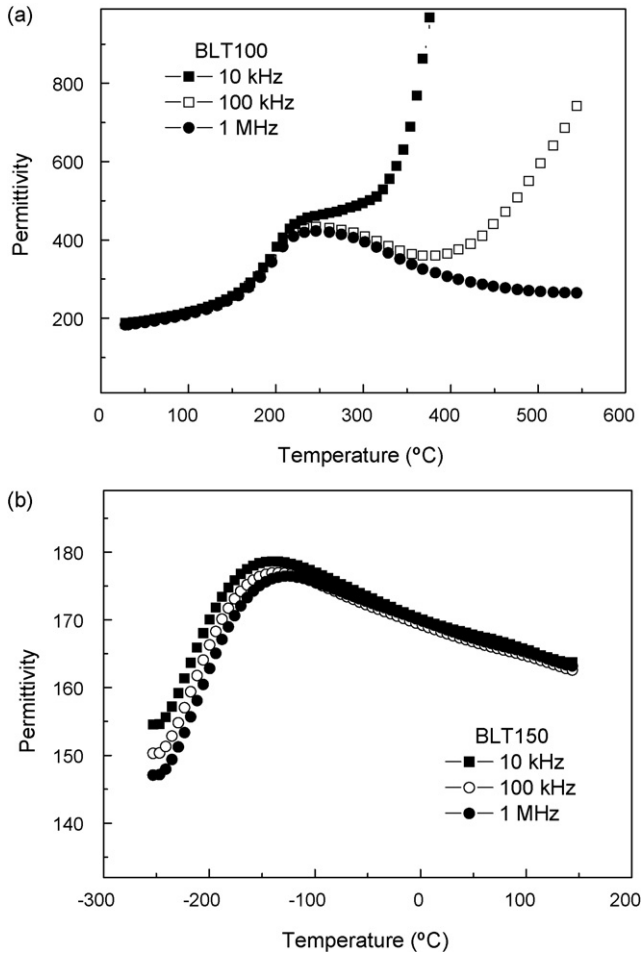

Fig. 9. Temperature dependence of permittivity from the (a) BLT100 ($x = 1.0$) and (b) BLT150 ($x = 1.5$) samples at three different frequencies (10 kHz, 100 kHz and 1 MHz).

$x \leq 1.0$, while a relaxor (frequency-dependent) behavior characterized the phase transition for those BLT samples with $x > 1.0$. This observation agrees well with a previous similar statement in literature where the relaxor behavior in the BLT system was observed for $x \geq 1.25$.[9] Further, as is well known, the permittivity of ferroelectric materials should monotonically decreases above T_m as the measuring temperature increases (Curie–Weiss-like law). Presently, the observation of both (i) an increase of permittivity as well as (ii) a permittivity dispersion above the transition temperature for, respectively, BLT075 and BLT100 in Fig. 6 and BLT100 in Fig. 9a should arise from interfacial polarization processes most likely involving grain boundary-associated blocking effects of charge carriers during electric field-induced migration in the electrically heterogeneous medium.[23,24] In terms of fixed-frequency dielectric spectra from electroceramics, as found, such effects are well known to become resolvable especially towards higher temperatures.

4. Conclusions

Ceramics of $Bi_{4-x}La_xTi_3O_{12}$ were prepared and studied in this work. During sintering, La^{3+} was found to promote a

grain-boundary pinning process that reduces the material grain size, while changing the grain morphology from the classical plate-like form, typically observed in BIT ceramics, to a spherical-like form. In particular, starting from high-purity raw materials, the solubility limit (x_L) of La^{3+} into BIT was found to locate slightly above $x = 1.5$, that is, below an earlier value of $x_L = 2.8$ previously reported in the literature. On the other hand, within the solid solution solubility region here detected, it is observed that the ferro- to para-electric transition temperature (T_m) of the BLT system decreases monotonically but not linearly with La^{3+}, while inducing this rare-earth cation a relaxor permittivity–temperature behavior around T_m for compositions above $x = 1.0$. The values of permittivity and dielectric losses processed in this work compare well with those typical values reported elsewhere for BIT-based ferroelectric ceramics.

Acknowledgments

The authors gratefully acknowledge financial support from FAPESP and CNPq, two Brazilian research-funding agencies and Dr. Michel Venet for some of the electrical measurements carried out.

References

1. Herbert, J. M., *Ferroelectric Transducers and Sensors*. Gordon and Breach Science Publishers, New York, 1982.
2. Xu, Y., *Ferroelectric Materials and Their Applications*. Elsevier Science Publishers, 1991.
3. Park, B. H., Kang, B. S., Bu, S. D., Noh, T. W., Lee, J. and Jo, W., Lanthanum-substituted bismuth titanate for use in non-volatile memories. *Nature*, 1999, **401**, 682–684.
4. Wolfe, R. W. and Newnham, R. E., Rare earth bismuth titanates. *J. Electrochem. Soc.*, 1969, **116**, 832–835.
5. Armstrong, R. A. and Newnham, R. E., Bismuth titanate solid solutions. *Mater. Res. Bull.*, 1972, **7**, 1025–1034.
6. Shimazu, M., Tanaka, J., Muramatsu, K. and Tsukioka, M., Phase transition in the family $La_xBi_{4-x}Ti_3O_{12}$: in relation to lattice symmetry and distortion. *J. Solid State Chem.*, 1980, **35**, 402–406.
7. Takenaka, T. and Sakata, K., Electrical properties of grain-oriented ferroelectric ceramics in some lanthanum modified layer-structure oxides. *Ferroelectrics*, 1981, **38**, 769–772.
8. Chu, M.-W., Caldes, M. T., Piffard, Y., Marie, A.-M., Gautier, E., Joubert, O. *et al.*, Evidence for a monoclinic distortion in the ferroelectric Aurivillius phase $Bi_3LaTi_3O_{12}$. *J. Solid State Chem.*, 2003, **172**, 389–395.
9. Chen, X.-B., Hui, R., Zhu, J., Lu, W.-P. and Mao, X.-Y., Relaxor properties of lanthanum-doped bismuth layer-structured ferroelectrics. *J. Appl. Phys.*, 2004, **96**, 5697–5700.
10. Macedo, Z. S., Ferrari, C. R. and Hernandes, A. C., Impedance spectroscopy of $Bi_4Ti_3O_{12}$ ceramic produced by self-propagating high-temperature synthesis technique. *J. Eur. Ceram. Soc.*, 2004, **24**, 2567–2574.
11. Patwardhan, J. S. and Rahaman, M. N., Compositional effects on densification and microstructural evolution of bismuth titanate. *J. Mater. Sci.*, 2004, **39**, 133–139.
12. Su, W.-F. and Lu, Y.-T., Synthesis, phase transformation and dielectric properties of sol–gel derived $Bi_2Ti_2O_7$ ceramics. *Mater. Chem. Phys.*, 2003, **80**, 632–637.
13. Mendelson, M. I., Average grain size in polycrystalline ceramics. *J. Am. Ceram. Soc.*, 1969, **52**, 443–446.
14. Kan, Y., Jin, X., Zhang, G., Wang, P., Cheng, Y.-B. and Yan, D., Lanthanum modified bismuth titanate prepared by a hydrolysis method. *J. Mater. Chem.*, 2004, **14**, 3566–3570.
15. Lin, T.-F. and Hu, C.-T., Influence of stoichiometry on the microstructure and positive temperature coefficient of resistivity of semiconducting barium titanate ceramics. *J. Am. Ceram. Soc.*, 1990, **73**, 531–536.
16. Lee, H.-Y. and Freer, R., The mechanism of abnormal grain growth in $Sr_{0.6}Ba_{0.4}Nb_2O_6$ ceramics. *J. Appl. Phys.*, 1997, **81**, 376–382.
17. Kim, J. S., Ahn, C. W., Lee, H. J., Kim, I. W. and Jin, B. M., Nb doping effects on ferroelectric and electrical properties of ferroelectric $Bi_{3.25}La_{0.75}(Ti_{1-x}Nb_x)_3O_{12}$ ceramics. *Ceram. Int.*, 2004, **30**, 1459–1462.
18. Hervoches, C. H. and Lightfoot, P., A variable-temperature powder neutron diffraction study of ferroelectric $Bi_4Ti_3O_{12}$. *Chem. Mater.*, 1999, **11**, 3359–3364.
19. Rae, A. D., Thompson, J. G., Withers, R. L. and Willis, A. C., Structure refinement of commensurately modulated bismuth titanate, $Bi_4Ti_3O_{12}$. *Acta Cryst. B*, 1990, **46**, 474–487.
20. Jeon, M. K., Kim, Y.-I., Nahm, S.-H. and Woo, S. I., Combined structural refinement of $Bi_{3.5}La_{0.5}Ti_3O_{12}$ using neutron and X-ray powder diffraction data. *J. Phys. Chem. B*, 2005, **109**, 968–972.
21. Le Bail, A., Duroy, H. and Fourquet, J. L., Ab initio structure determination of $LiSbWO_6$ by X-ray powder diffraction. *Mater. Res. Bull.*, 1988, **23**, 447–452.
22. Cullity, B. D., *Elements of X-ray Diffraction* (*2nd. ed.*). Addison-Wesley Publishing Company, Inc., 1978.
23. M'Peko, J.-C., Portelles, J., Calderón, F. and Rodríguez, G., Dielectric anomaly and low frequency dispersion in ferroelectric materials at high temperatures. *J. Mater. Sci.*, 1998, **33**, 1633–1637.
24. Antonelli, E., M'Peko, J.-C. and Hernandes, A. C., Grain boundary-modified dielectric spectra of electroceramics: the occurrence of 'unexpected' thermal dielectric loss peaks. *Phys. Stat. Sol. (b)*, 2007, **244**, 3390–3397.